frontiers | Frontiers in Pharmacology

TYPE Original Research
PUBLISHED 14 February 2024
DOI 10.3389/fphar.2024.1303732

OPEN ACCESS

EDITED BY
Hong Duan,
Sichuan University, China

REVIEWED BY
Muhammad Khan,
University of the Punjab, Pakistan
Xiao Wang,
Jinan University, China
Birandra Kumar Sinha,
National Institute of Environmental Health Sciences (NIH), United States

*CORRESPONDENCE
Jingmin Zhang,
fcczhangjm@zzu.edu.cn
Yuna Chai,
yuna999@126.com

†These authors have contributed equally to this work and share first authorship

RECEIVED 28 September 2023
ACCEPTED 25 January 2024
PUBLISHED 14 February 2024

CITATION
Wang X, Ding R, Fu Z, Yang M, Li D, Zhou Y, Qin C, Zhang W, Si L, Zhang J and Chai Y (2024), Overexpression of miR-506-3p reversed doxorubicin resistance in drug-resistant osteosarcoma cells.
Front. Pharmacol. 15:1303732.
doi: 10.3389/fphar.2024.1303732

Overexpression of miR-506-3p reversed doxorubicin resistance in drug-resistant osteosarcoma cells

Xinru Wang[1†], Rumeng Ding[1†], Zhe Fu[2], Meng Yang[1], Duolu Li[1], Yubing Zhou[1], Chongzhen Qin[1], Wenda Zhang[1], Liuzhe Si[1], Jingmin Zhang[1*] and Yuna Chai[1*]

[1]Department of Pharmacy, The First Affiliated Hospital of Zhengzhou University, Zhengzhou, Henan, China, [2]Department of General Surgery, The Third Affiliated Hospital of Zhengzhou University, Zhengzhou, Henan, China

Background and objective: Osteosarcoma is a common primary malignant tumor of bone, and doxorubicin is one of the most widely used therapeutic drugs. While the problem of doxorubicin resistance limits the long-term treatment benefits in osteosarcoma patients. The role of miRNAs and their target genes in osteosarcoma have become increasingly prominent. Currently, there is no report on miR-506-3p reversing doxorubicin resistance by targeting STAT3 in osteosarcoma. The purpose of this study was to investigate the molecular mechanism that overexpression of miR-506-3p reverses doxorubicin resistance in drug-resistant osteosarcoma cells.

Methods: Doxorubicin-resistant osteosarcoma cells (U-2OS/Dox) were constructed by intermittent stepwise increasing stoichiometry. The target genes of miR-506-3p were predicted by bioinformatics approach and the targeting relationship between miR-506-3p and STAT3 was detected using dual luciferase reporter assay. U-2OS/Dox cells were treated with miR-506-3p overexpression and STAT3 silencing respectively. Then Western blot and RT-qPCR were used to detect the protein and mRNA expression levels of JAK2/STAT3 signaling pathway, drug-resistant and apoptotic associated molecules. The migration and invasion were assessed by cell scratch assay and transwell assay. The cell proliferative viability and apoptosis were investigated by CCK8 assay and flow cytometry assay.

Results: U-2OS/Dox cells were successfully constructed with a 14.4-fold resistance. MiR-506-3p is directly bound to the 3′-UTR of STAT3 mRNA. Compared with U-2OS cells, the mRNA expression of miR-506-3p was reduced in U-2OS/Dox cells. Overexpression of miR-506-3p decreased the mRNA expression levels of JAK2, STAT3, MDR1/ABCB1, MRP1/ABCC1, Survivin and Bcl-2, and decreased the protein expression levels of p-JAK2, STAT3, MDR1/ABCB1, MRP1/ABCC1, Survivin and Bcl-2, and conversely increased Bax expression. It also inhibited the proliferation, migration and invasion of U-2OS/Dox cells and promoted cells apoptosis. The results of STAT3 silencing experiments in the above indicators were consistent with that of miR-506-3p overexpression.

Conclusion: Overexpression of miR-506-3p could inhibit the JAK2/STAT3 pathway and the malignant biological behaviors, then further reverse

doxorubicin resistance in drug-resistant osteosarcoma cells. The study reported a new molecular mechanism for reversing the resistance of osteosarcoma to doxorubicin chemotherapy and provided theoretical support for solving the clinical problems of doxorubicin resistance in osteosarcoma.

KEYWORDS

osteosarcoma, doxorubicin resistance, miR-506-3p, JAK2/STAT3 signaling pathway, U-2OS/Dox

1 Introduction

As a highly aggressive bone malignancy, osteosarcoma was the most common primary tumor originating from mesenchymal cells, with a high prevalence in adolescents aged 10–14 years and older adults over the age of 60 years (Fu et al., 2023). Currently, the first-line treatment for osteosarcoma includes surgery, radiotherapy and chemotherapy. Although the 5-year survival rate has improved, the treatment for advanced and recurrent patients is still unsatisfactory. Osteosarcoma only responds to high doses of chemotherapeutic agents and is highly susceptible to chemoresistance, which are the main reasons for poor prognosis in osteosarcoma patients. Moreover, for osteosarcoma patients who develop chemotherapy resistance, the overall 5-year survival rate was significantly reduced to less than 20% (Zhu et al., 2019). Chemotherapy resistance was detrimental to subsequent treatment plans for patients, and was one of the difficulties in treatment for the orthopedic community. Therefore, it is urgent to solve the problem of chemoresistance in osteosarcoma patients.

During the treatment for osteosarcoma, chemoresistance is the most important pathophysiological basis for malignant tumor proliferation, susceptibility to recurrence and metastasis. The mechanism of chemoresistance in osteosarcoma has not been fully elucidated. Possible mechanisms included alteration of the activity of DNA topoisomerase, increase in the activity of glutathione transferase, dysfunction of membrane transport, activation of autophagy, and enhancement of DNA damage repair, etc (Lilienthal and Herold, 2020). Currently, doxorubicin, also known as adriamycin, is the cornerstone of osteosarcoma treatment, and had a response rate of up to 40% on osteosarcoma (Chou and Gorlick, 2006). However, long-term use of doxorubicin can lead to drug resistance. The occurrence of resistance could be caused by a variety of factors, and relevant pathogenesis is mainly concentrated in the key membrane transport proteins including P-gP, MDR1/ABCB1, and MRP1/ABCC1 (Elfadadny et al., 2021).

As a confluence of many oncogenic signaling pathways, the activation of signal transducer and activator of transcription 3 (STAT3) could induce aberrant expression of genes associated with tumor cell proliferation, differentiation, apoptosis, and chemo-resistance, and thus promoted tumor transformation, causing poor prognosis in patients (Barre et al., 2007; Hu et al., 2019). JAK2/STAT3 is a classical signaling pathway in tumor research. Under normal physiological conditions, transient activation of JAK2/STAT3 is strictly regulated. However, sustained activation of JAK2/STAT3 signaling had been found in many solid tumors, such as breast cancer, which promoted solid tumorigenesis, tumor growth, angiogenesis, host immune evasion, apoptosis resistance, carcinogenesis, and metastasis (Yu et al., 2009; Mengie Ayele et al., 2022; Rah et al., 2022). It had been demonstrated that the inhibition of JAK2/STAT3 signaling pathway could decrease cell viability, invasion and migration of osteosarcoma cells and induced apoptosis in cancer cells (Jia et al., 2022; Li and Liu, 2023; Ma et al., 2023). In addition, doxorubicin resistance could be antagonized by blocking the activation of the JAK2/STAT3 pathway induced by IL-6 secretion (Lu et al., 2021). However, the profound mechanism of reversing doxorubicin resistance mediated by the STAT3 remains to be further discovered.

In recent years, great progress had been made in the study of tumor phenotype changes caused by the interaction of miRNA and target genes. Some studies had reported that miR-506 could inhibit the biological activity of glioma cells (Peng et al., 2016), human hepatocellular carcinoma cells (Su et al., 2019) and colorectal cancer cells (Wei et al., 2019) by targeting STAT3. MiR-506 was lowly expressed in osteosarcoma tissues, and upregulation of miR-506 level could inhibit osteosarcoma cell proliferation and invasion, and promoted osteosarcoma cell apoptosis (Yao et al., 2016; Hu et al., 2017; Jiashi et al., 2018; Li et al., 2021). So far, the role of miR-506-3p reversing doxorubicin resistance by regulating STAT3 in osteosarcoma has not been reported. In this study, we focused on investigating the mechanisms of miR-506-3p reversing doxorubicin resistance in osteosarcoma, and provided theoretical support for solving the clinical problems of doxorubicin resistance in osteosarcoma.

2 Results

2.1 Construction of drug-resistant osteosarcoma cell line

The half inhibitory concentration (IC_{50}) values of drug-sensitive osteosarcoma cells (U-2OS) and doxorubicin-resistant human osteosarcoma cell line (U-2OS/Dox) were 2.01 μg/mL and 29.00 μg/mL, respectively. The resistance index (RI) was 14.4-fold (Figures 1A, B, $p < 0.05$). The mRNA and protein expression levels of MDR1 in U-2OS/Dox cells were significantly upregulated (Figures 1C, D, $p < 0.01$). The results from cell counting kit-8 (CCK8) and Western blot assays demonstrated that U-2OS/Dox was successfully constructed.

2.2 Results of bioinformatics analysis

2.2.1 Target prediction of miR-506-3p

The results of the cancer genome atlas (TCGA) database analysis showed that the change trends of miR-506-3p in different cancer

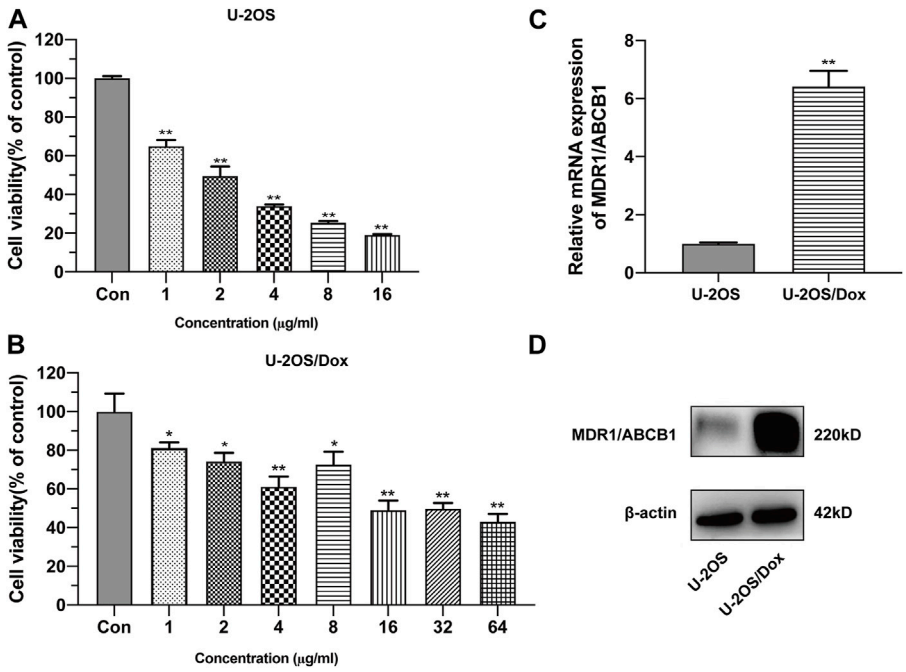

FIGURE 1
Construction of human osteosarcoma doxorubicin-resistant cell line U-2OS/Dox. The cell viability of drug-sensitive osteosarcoma cells U-2OS **(A)** and drug-resistant osteosarcoma cells U-2OS/Dox **(B)** were detected by CCK-8 assay with different concentrations of doxorubicin. IC_{50} values were detected in U-2OS (IC_{50} = 2.01 μg/mL) and in U-2OS/Dox (IC_{50} = 29.00 μg/mL) by CCK8 assay, RI = 14.4 fold. **(C, D)** The mRNA and protein expression levels of MDR1/ABCB1 in U-2OS and U-2OS/Dox were detected through RT-qPCR and Western blot, showing that MDR1/ABCB1 was significantly upregulated in U-2OS/Dox. *: $p < 0.05$, **: $p < 0.01$.

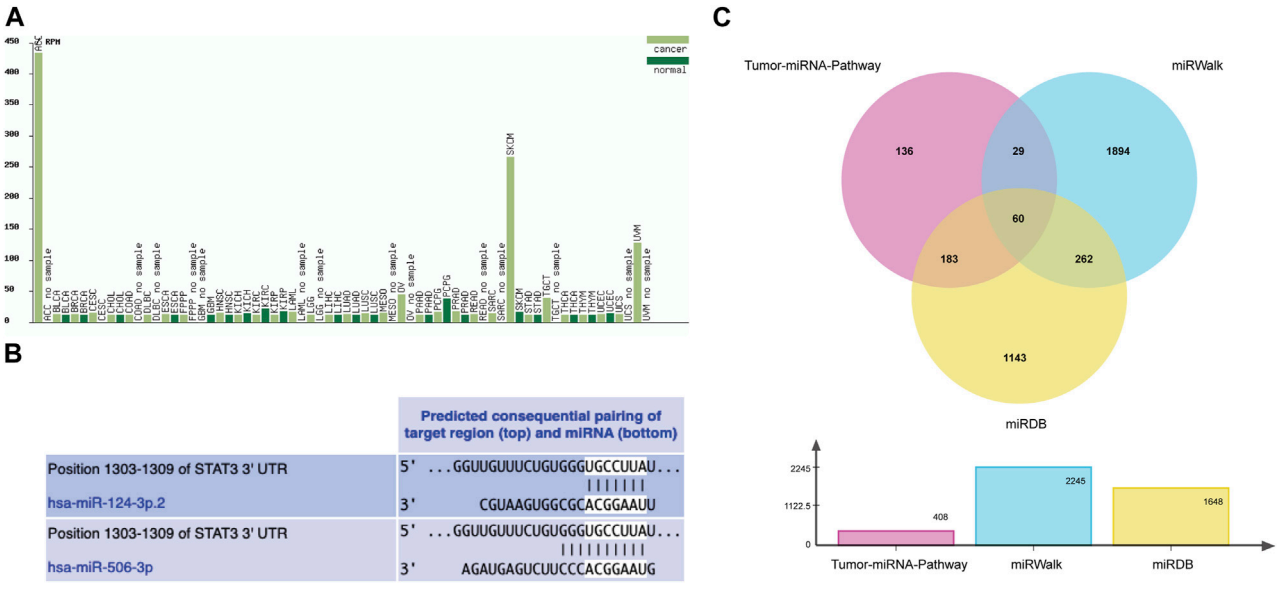

FIGURE 2
Tumor expression profile of miR-506-3p and prediction of binding sites and target mRNAs **(A)** Expression profiles of miR-506-3p in different tumor tissues and their paracancerous tissues, lacking the expression level of miR-506-3p in osteosarcoma. **(B)** The seed sequence of hsa-miR-506-3p was found to coincide with that of hsa-miR-124 by TargetScan Human 8.0 software prediction. **(C)** The Venn diagram of target genes prediction regulated by miR-506-3p in three databases.

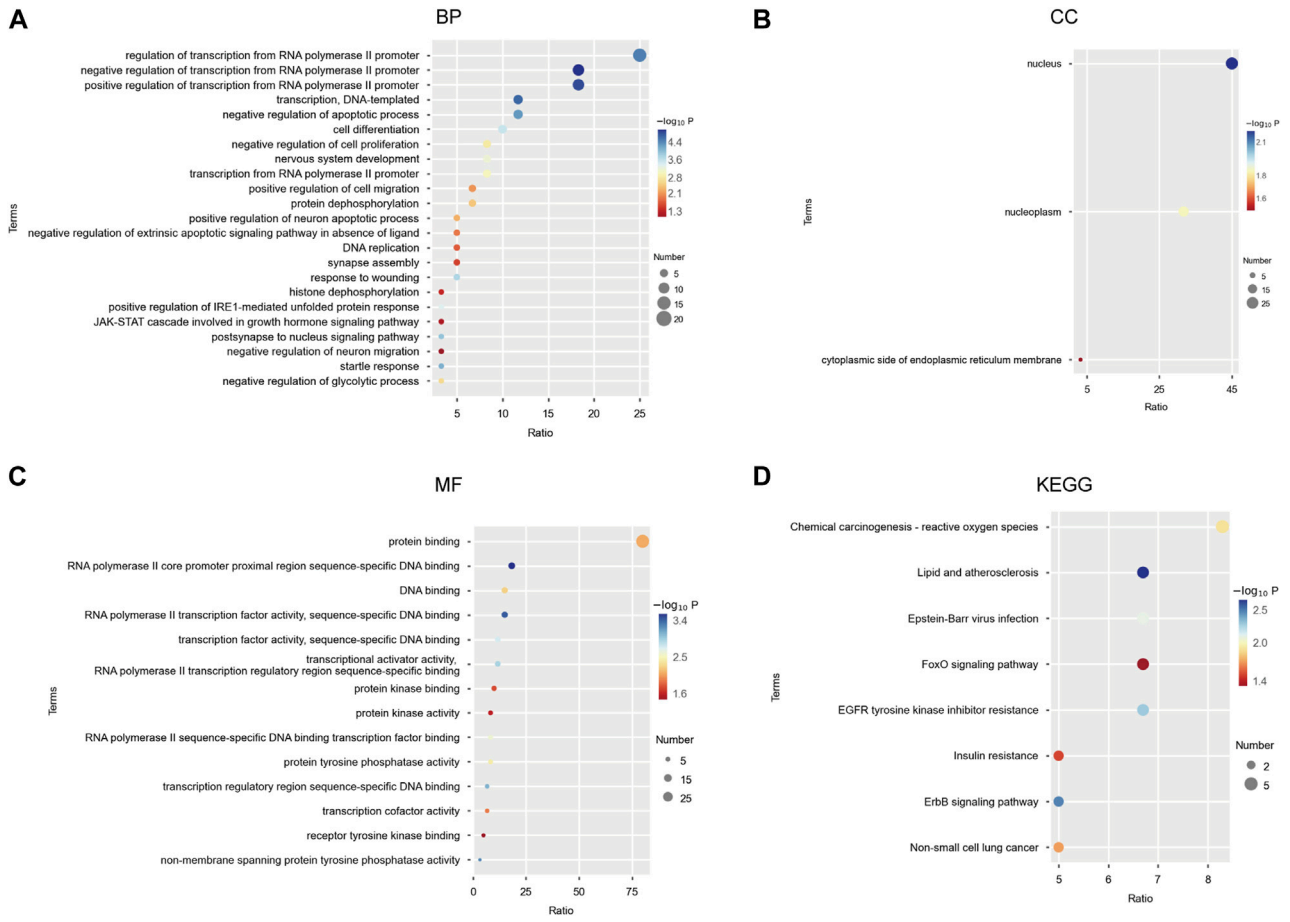

FIGURE 3
GO functional and KEGG pathway enrichment analysis of miR-506-3p target mRNAs **(A)** Twenty-three biological processes (BP) associated with miR-506-3p target genes and gene products by GO enrichment analysis; **(B)** Three cellular components (CC) associated with miR-506-3p target genes by GO enrichment analysis; **(C)** Fourteen molecular functions (MF) associated with miR-506-3p target genes by GO enrichment analysis. **(D)** Eight important signaling pathways associated with miR-506-3p target genes by KEGG enrichment analysis.

types were not consistent, as shown in Figure 2A. However, the database lacks findings on the miR-506-3p in osteosarcoma, so this study explored the expression level of miR-506-3p in drug-sensitive and drug-resistant cells.

As predicted by TargetScan Human 8.0 database, the seed sequences of miR-506-3p and miR-124 tended to be consistent. Moreover, the binding site predicted by the 3′-UTR of miR-506-3p was broadly conserved with that of miR-124, as shown in Figure 2B.

From the Tumor-miRNA-Pathway database 408 genes were found, 1648 targets from the miRWalk database and 2245 genes from the miRDB database. Taking the intersection form by Wayne's analysis finally yielded 60 genes, and STAT3 was one of the target genes that miR-506-3p might regulate, as shown in Figure 2C.

2.2.2 GO and KEGG enrichment analysis of miR-506-3p target genes

We performed Gene Ontology (GO) and Kyoto Encyclopedia of Genomes (KEGG) pathway enrichment analysis of miR-506-3p predicted target genes. Among them, GO enrichment analysis was used to characterize the relevant biological processes (BP), cellular components (CC) and molecular functions (MF). We observed that these target genes significantly clustered 23 terms in BP, 3 terms in CC, and 14 terms in MF (Figures 3A–C). They might be involved in apoptosis, cell proliferation and cell migration, which were mediated by transcriptional activator or tyrosine kinase signaling pathways, including the JAK-STAT. KEGG enrichment analysis identified eight important signaling pathways (Figure 3D), including the chemical carcinogenesis-reactive oxygen species signaling pathway, the Forkhead Box O (FoxO) signaling pathway, the epidermal growth factor receptor-tyrosine kinase inhibitor (EGFR-TKI) drug resistance signaling pathway, and the receptor protein-tyrosine kinase (ErbB) signaling pathway, etc.

2.2.3 Protein-protein interaction (PPI) networks of miR-506-3p target genes

The STRING database was utilized to screen the target genes of miR-506-3p. PPI networks were established (Figure 4A), and then, were imported into Cytoscape software. The key genes targeted by miR-506-3p were acquired through the cytoHubba plug-in, including STAT3, RAC-beta serine/threonine-protein kinase (AKT2), B-cell lymphoma 2-like 11 (BCL2L11), Myocyte enhancer factor 2A (MEF2A), Recombinant superoxide dismutase 2 (SOD2), Frataxin (FXN), and

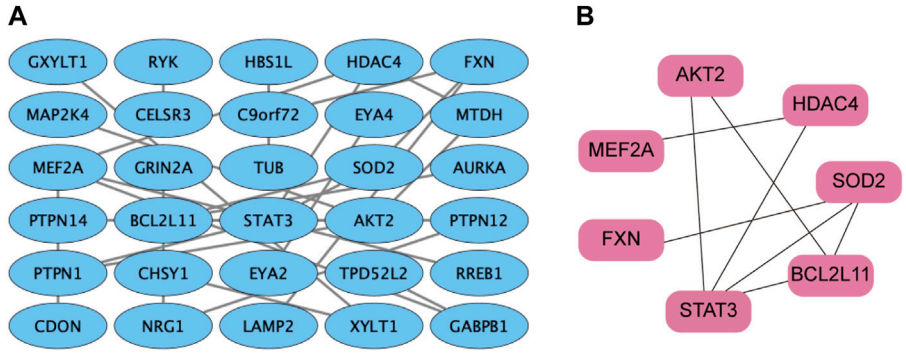

FIGURE 4
PPI network of miR-506-3p target genes **(A)** PPI network of miR-506-3p target genes were constructed by the STRING database. **(B)** The key genes targeted by miR-506-3p, including seven pivotal target genes, namely, STAT3, AKT2, BCL2L11, MEF2A, SOD2, FXN and HDAC4 were screened out by the cytoHubba plug-in and degree topology algorithm in Cytoscape software (version 3.8.0).

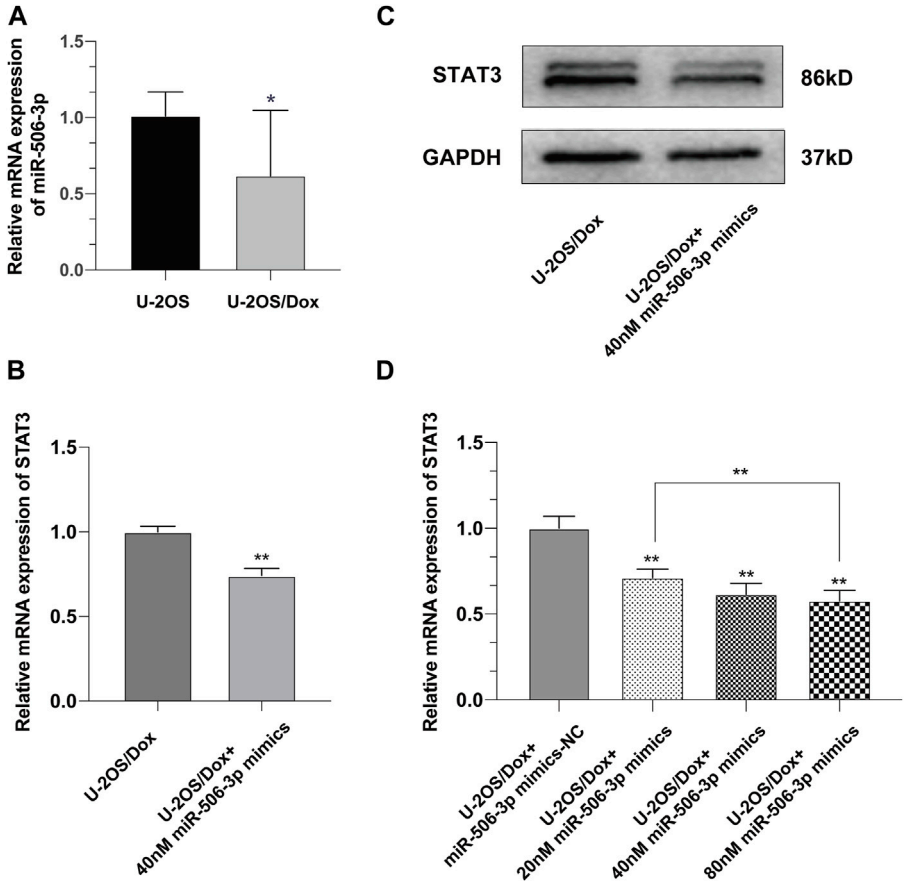

FIGURE 5
Overexpression of miR-506-3p downregulated the expression of STAT3 in U-2OS/Dox **(A)** The expression level of miR-506-3p in osteosarcoma-resistant cell line U-2OS/Dox was significantly lower than that in its parental cell line U-2OS. **(B, C)** The mRNA and protein expression levels of STAT3 were downregulated after transfection of 40 nM miR-506-3p mimics in U-2OS/Dox cells. **(D)** The inhibitory effect of miR-506-3p mimics on STAT3 was enhanced with the increasing concentration of miR-506-3p mimics. *: $p < 0.05$, **: $p < 0.01$.

Histone deacetylase 4 (HDAC4) (Figure 4B), which are hub target genes that may be involved in regulating osteosarcoma development and the molecular mechanisms of chemoresistance. Our previous studies found that the inhibition of STAT3 expression could reverse the chemosensitivity of osteosarcoma cells to doxorubicin, the STAT3 gene was chosen as a candidate target of miR-506-3p for the study of the molecular mechanism of reversing doxorubicin chemoresistance in drug-resistant osteosarcoma cells.

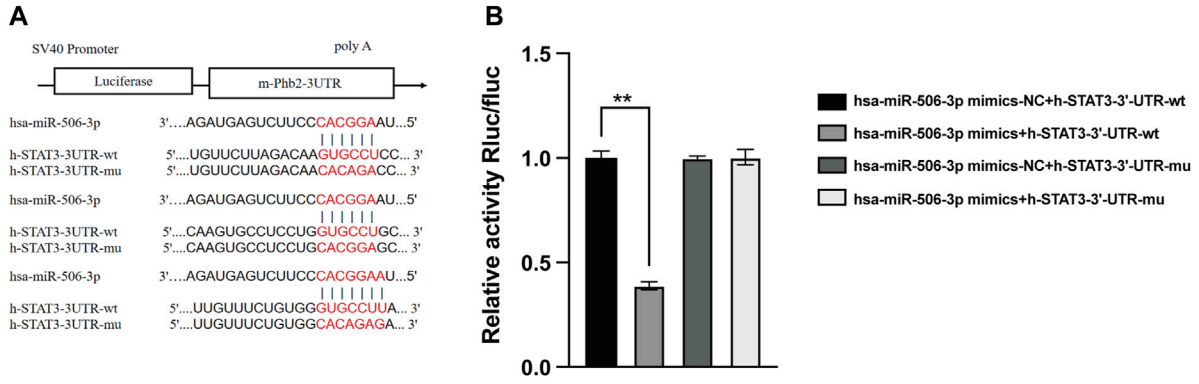

FIGURE 6
MiR-506-3p targeting STAT3 by dual luciferase reporter gene assay **(A)** Prediction of potential binding sites of miR-506-3p to the 3′-UTR of STAT3. **(B)** Dual luciferase reporter gene assay showed a significant decrease in the relative activity of STAT3 wild-type luciferase-expressing vectors. **: $p < 0.01$.

2.3 MiR-506-3p suppressed STAT3 expression by directly targeting the STAT3 3′-UTR

Real time quantitative polymerase chain reaction (RT-qPCR) results showed that the expression level of miR-506-3p in U-2OS/Dox was significantly lower than that in its parental cell line U-2OS (Figure 5A, $p < 0.05$). After transfection of U-2OS/Dox cells with miR-506-3p mimics, we found that transfection of 40 nM miR-506-3p mimics downregulated STAT3 expression at the mRNA and protein levels (Figures 5B, C, $p < 0.01$). With the increasing concentration of miR-506-3p mimics, its inhibitory effect on STAT3 was also gradually enhanced (Figure 5D, $p < 0.01$). It indicated that miR-506-3p was negatively correlated with STAT3 expression in U-2OS/Dox cells relative to U-2OS, and overexpression of miR-506-3p inhibited STAT3 expression in U-2OS/Dox cells.

As verified by the dual luciferase reporter gene assay, the relative activity of STAT3 wild-type luciferase expression vector was significantly decreased to 0.291 ± 0.014 after transfection with miR-506-3p mimics, whereas that of the other three controls was 0.748 ± 0.025, 0.743 ± 0.007 and 0.746 ± 0.028 (Figure 6, $p < 0.01$). It could be seen that miR-506-3p bound directly to STAT3 3′-untranslated region (3′-UTR), indicating that there may be a targeted regulatory relationship between miR-506-3p and STAT3.

2.4 Effects of miR-506-3p overexpression and STAT3 silencing on migration and invasion of U-2OS/Dox cells

MiR-506-3p mimics and mimics-NC were transfected into U-2OS/Dox cells using liposome transfection technology. RT-qPCR assay of the transfection efficiency showed that the miR-506-3p expression level in the mimics group was significantly higher than that in the control and mimics-NC groups, indicating successful transfection (Figure 7A, $p < 0.01$). The gene silencing technology was utilized to cause low expression of STAT3 in U-2OS/Dox cells. RT-qPCR and Western blot experiments showed that the expression level of STAT3 in the STAT3-siRNA1 group was significantly reduced compared with that in the STAT3-siRNA-NC group, STAT3-siRNA2 and STAT3-siRNA3 (Figures 7B–D, $p < 0.05$). Thereby, STAT3-siRNA1 had the best effect on gene silencing among all the groups tested and was chosen for the following experiments.

The results showed that after doxorubicin was added to each group (U-2OS/Dox group, U-2OS/Dox + miR-506-3p mimics-NC group, U-2OS/Dox + miR-506-3p mimics group, U-2OS/Dox + STAT3-siRNA-NC group and U-2OS/Dox + STAT3-siRNA1 group), compared with the control group (U-2OS/Dox + Dox), the numbers of migrating cells (Figure 8, $p < 0.05$) and invading cells (Figure 9, $p < 0.05$) were significantly reduced in the miR-506-3p overexpressing group (U-2OS/Dox + miR-506-3p mimics) and STAT3 silencing group (U-2OS/Dox + STAT3-siRNA1).

2.5 Effects of miR-506-3p overexpression and STAT3 silencing on proliferation and apoptosis of U-2OS/Dox cells

After the U-2OS/Dox cells in each group were co-cultured with 29 μg/mL doxorubicin for 24 h, 48 h and 72 h, through CCK8 test, the cell proliferation activities in the overexpression miR-506-3p group and the STAT3 silencing group were significantly reduced compared with the control group (Figure 10, $p < 0.05$). Flow cytometry results showed that the apoptosis rate was significantly higher in the miR-506-3p overexpression group and the of STAT3 silencing group (Figures 11A, B, $p < 0.01$). The expressions of anti-apoptotic proteins Survivin and B-cell lymphoma-2 (Bcl-2) were detected by Western blot and RT-qPCR, and the results showed that the expressions of Survivin (Figures 11C, E) and Bcl-2 (Figures 11C, G) were significantly reduced in the miR-506-3p overexpression group and the STAT3 silencing group. The protein (Figure 11C) and mRNA (Figure 11F) expression levels of pro-apoptotic protein Bcl-2 associated X (Bax) were significantly increased. The relative protein expression ratio of Bcl-2/Bax was significantly reduced in the overexpression of miR-506-3p group and the silencing STAT3 group (Figure 11D, $p < 0.01$). The results above indicated that overexpression of miR-506-3p inhibited U-2OS/Dox cell

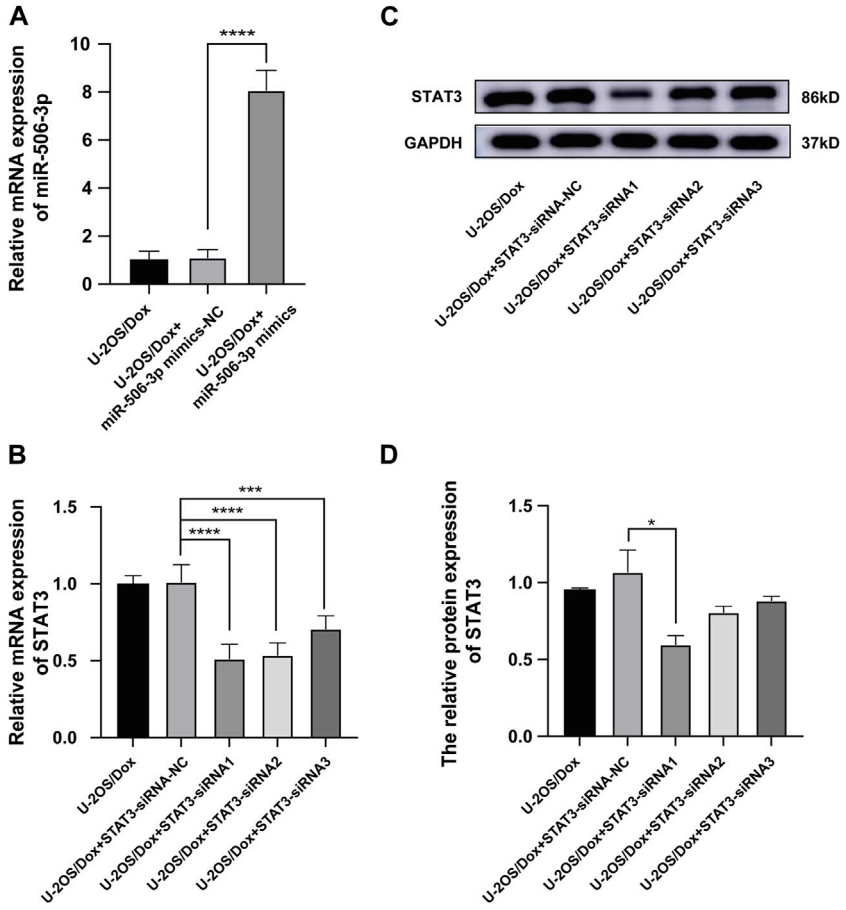

FIGURE 7
The Screening of STAT3 siRNAs **(A)** The miR-506-3p expression level in U-2OS/Dox + miR-506-3p mimics group was significantly higher than that in the U-2OS/Dox control group or U-2OS/Dox + miR-506-3p mimics-NC group by RT-qPCR detection, indicating that transfection was successful. **(B–D)** STAT3-siRNA1 had the best silencing effect on STAT3 gene by RT-qPCR and Western blot experiments. *: $p < 0.05$, **: $p < 0.01$.

proliferation and promoted U-2OS/Dox cell apoptosis, consistent with the effects of silencing STAT3.

2.6 Effects of miR-506-3p overexpression and STAT3 silencing on drug resistance pathway proteins in U-2OS/Dox cells

After doxorubicin was added to each group (U-2OS group, U-2OS/Dox group, U-2OS/Dox + STAT3-siRNA-NC group, U-2OS/Dox + STAT3-siRNA1 group, U-2OS/Dox + miR-506-3p mimics-NC group and U-2OS/Dox + miR-506-3p mimics group), compared with the U-2OS/Dox + Dox group, the mRNA expression levels of JAK2, STAT3, MRP1/ABCC1 and MDR1/ABCB1 were all remarkably inhibited in the miR-506-3p overexpression group and the STAT3 silencing group (Figures 12A–D, $p < 0.01$). However, at the protein expression level, overexpression of miR-506-3p and silencing of STAT3 significantly reduced the expression levels of p-JAK2/JAK2 (Figures 12E, F, $p < 0.05$) and STAT3 protein (Figures 12E, I, $p < 0.05$), which also reduced the expression levels of p-STAT3/STAT3 (Figures 12E, G) and JAK2 protein (Figures 12E, H), but there was no statistically significant difference. The results suggested that miR-506-3p overexpression inhibited the JAK2/STAT3 signaling pathway, thereby reversed the chemoresistance of U-2OS/Dox cells to doxorubicin, consistent with the results of STAT3 silencing.

3 Discussion

Currently, chemotherapy had become one of the mainstream treatments for osteosarcoma. MAP, consisting of methotrexate, doxorubicin and cisplatin, was the most widely available chemotherapy regimen for osteosarcoma (Hu et al., 2022). Unfortunately, some osteosarcoma patients showed poor chemosensitivity to these antitumor agents, and they were prone to chemoresistance during treatment, even with rising dose, shortening the period of chemotherapy or changing interval with other anticancer drugs. These patients still could not avoid recurrence and metastasis (Xiao et al., 2018). Doxorubicin, as the first-line drug for osteosarcoma, could induce osteosarcoma cell apoptosis and activated host immune response against tumor-specific antigens (Hattinger et al., 2015). However, due to serious drug resistance issues, osteosarcoma patients were greatly limited in their choice of regimens.

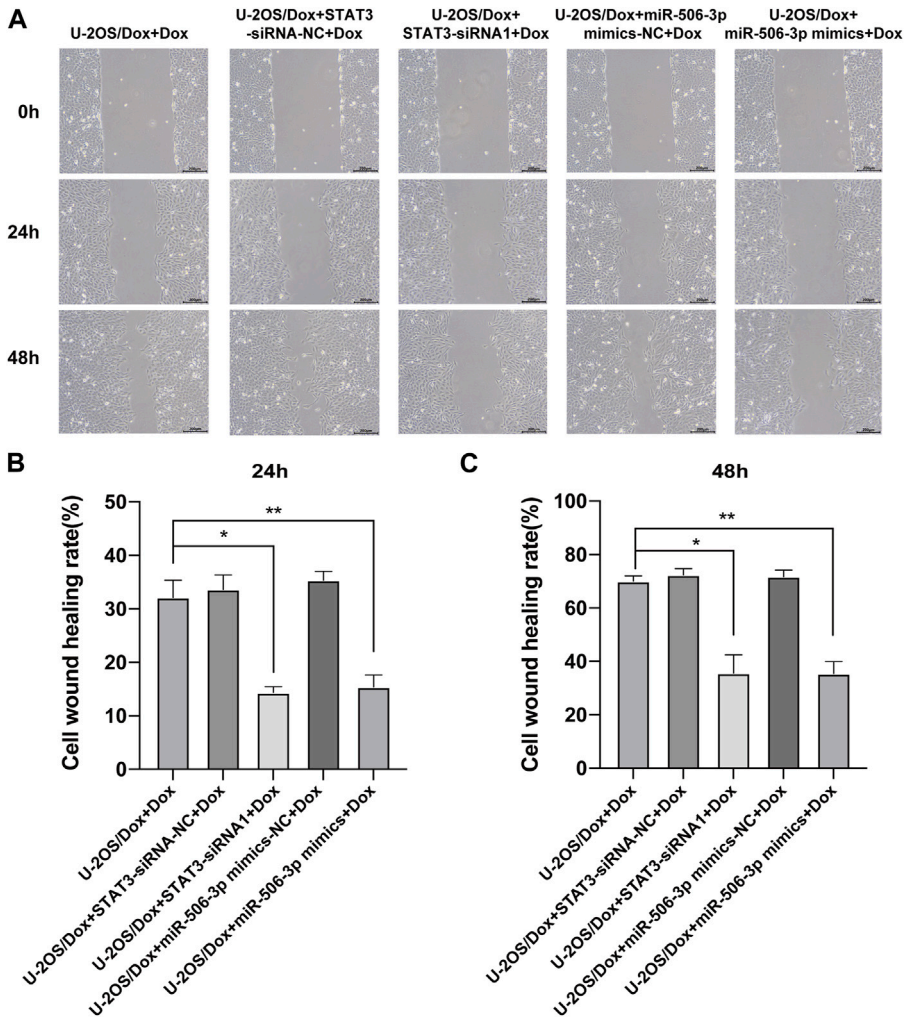

FIGURE 8
The migratory abilities of drug-resistant osteosarcoma cells were both inhibited by miR-506-3p overexpression and silencing STAT3 **(A)** The cell healing images of scratches at 0 h, 24 h or 48 h by cell scratching assay (magnification, ×100). The number of migrated cells in the U-2OS/Dox were both significantly reduced in the overexpression of miR-506-3p group (U-2OS/Dox + miR-506-3p mimics) and the silencing of STAT3 group (U-2OS/Dox + STAT3-siRNA1) after 24 h **(B)** or 48 h **(C)** of co-culture, compared with the drug-resistant osteosarcoma cells spiked group (U-2OS/Dox + Dox). *: $p < 0.05$, **: $p < 0.01$.

STATs were a family of proteins that existed in the cytoplasm and could be translocated into the nucleus to bind to DNA upon activation, which had the dual functions of signal transduction and transcriptional regulation. STAT3, an important member of the family of STATs, had been recognized as an oncogene that was closely related to tumor development (Barton, 2006). Studies had shown that STAT3 was highly expressed and continuously activated in osteosarcoma, which was involved in various pathological processes such as cell transformation, proliferation, tumor formation, invasion, migration, immune escape and drug resistance (Salas et al., 2014; Zhang et al., 2017). Inhibition of STAT3 activity had been shown to improve the chemosensitivity of osteosarcoma cells (Wang et al., 2011; Liu et al., 2021). We found that silencing STAT3 inhibited the cells proliferation, migration, and invasion ability of U-2OS/Dox cells and promoted cells apoptosis.

Studies had demonstrated that there were a large number of differentially expressed miRNAs in osteosarcoma tissues and cell lines. Some of these miRNAs were related to the development of osteosarcoma, while others were involved in the regulation of drug resistance in osteosarcoma (Tang et al., 2021). High expression of miR-124 in tumor tissues was a favorable prognostic marker for osteosarcoma (Wang et al., 2016; Cong et al., 2018). Three other studies have confirmed that miR-124 could inhibit the protein expression of STAT3 by directly targeting the 3′-UTR that binds STAT3, thereby suppress the invasive and migratory ability of tumor cells and help to overcome chemoresistance (Hu et al., 2016; Liu et al., 2019; Qi et al., 2019). We found that the seed sequence of hsa-miR-506-3p converged with that of hsa-miR-124 by pre-bioinformatics analysis, and the predicted that the binding site of miR-506-3p to the 3′-UTR of target gene STAT3 was broadly conserved with miR-124. Therefore, we predict that miR-506-3p is also able to directly target STAT3. MiR-506-3p played an important role in malignant tumor proliferation, apoptosis, migration, invasion, and epithelial-mesenchymal transition (Wang et al., 2019; Li et al., 2020; Liu et al., 2020). Moreover, it was closely related to tumor resistance. MiR-506-3p mainly played

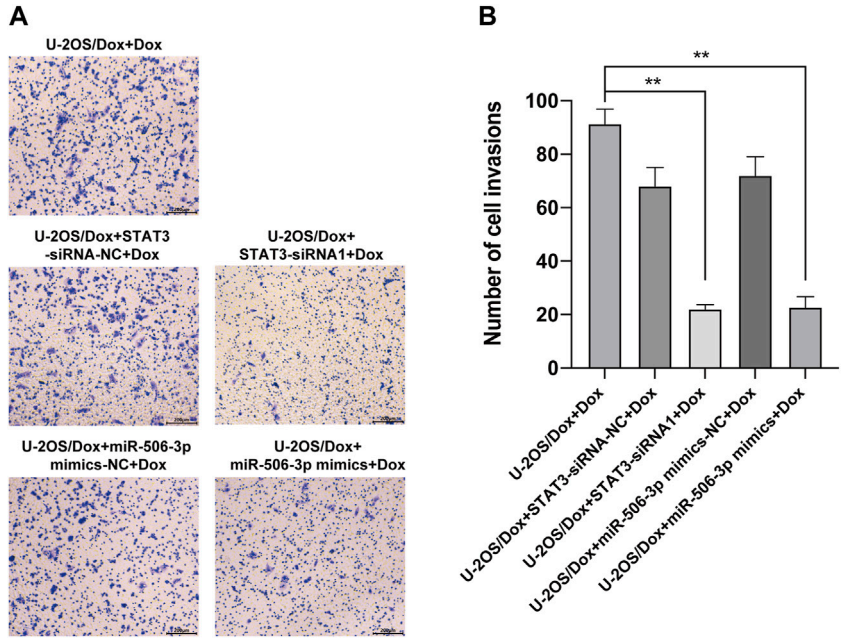

FIGURE 9
The invasive abilities of drug-resistant osteosarcoma cells were both inhibited by miR-506-3p overexpression and silencing STAT3 **(A)** The cell migration rates were detected by the transwell assay under an inverted microscope (magnification, ×100) after 24 h incubation. **(B)** The number of invasive cells in the U-2OS/Dox were both significantly reduced in the overexpression of miR-506-3p group (U-2OS/Dox + miR-506-3p mimics) and the silencing of STAT3 group (U-2OS/Dox + STAT3-siRNA1) after 24 h co-culture, compared with the drug-resistant osteosarcoma cells spiked group (U-2OS/Dox + Dox). *: $p < 0.05$.

an antitumor role, and could also increase the sensitivity of osteosarcoma to cisplatin (Dong and Qu, 2020). However, no studies have been reported on the role of miR-506-3p in the development of osteosarcoma and reversal of doxorubicin resistance by targeting STAT3. Our study found that miR-506-3p was significantly inhibited in U-2OS/Dox cells and further acquired the key target genes regulated by miR-506-3p, including STAT3. To fully understand the targeting relationship between miR-506-3p and STAT3, we performed dual luciferase reporter gene assay experiments, and demonstrated that there was a complementary binding sequence with miR-506-3p in the base sequence of STAT3 3′-UTR. In addition, the experimental results showed that overexpression of miR-506-3p reduced the STAT3 protein expression level in doxorubicin-resistant osteosarcoma cells U-2OS/Dox, indicating that miR-506-3p could inhibit the expression of STAT3 in osteosarcoma cells.

Tumor invasion and metastasis are complex processes regulated by multiple factors and multiple steps, involving tumor cells swimming out of the primary tumor, breaking through the basement membrane, passing through the cell stroma, entering blood vessels or lymphatic vessels, migrating to distant sites, finally colonizing and growing. The interactions of a variety of genes together formed a complex molecular biology network, which was the main biological feature of malignant tumors different from benign tumors (Hu et al., 2015; Chen et al., 2019). The effective control of proliferation, migration and invasion can inhibit the occurrence and development of tumors to a certain extent. It had been demonstrated that many miRNAs played a critical regulatory role in invasion and migration of osteosarcoma cells, including miR-506-3p (Jiashi et al., 2018). Our study also showed that overexpression of miR-506-3p inhibited the proliferation, migration and invasion of U-2OS/Dox cells, confirming that miR-506-3p plays an antitumor role in osteosarcoma.

Apoptosis was a tightly regulated cellular signaling process that occured via an extrinsic pathway of cell membrane death receptors and/or an intrinsic pathway dependent on mitochondria (Lossi, 2022). The Bcl-2 family played a key regulatory role in the extrinsic pathway of apoptosis, and consisted of pro-apoptotic proteins (such as Bax and Bak) and anti-apoptotic proteins (such as Bcl-2 and Bcl-xl). When the balance of anti-apoptotic and pro-apoptotic proteins in the Bcl-2 family was disrupted, it led to dysregulation of apoptosis (Wong, 2011). This defective apoptotic mechanism promoted the continued proliferation, angiogenesis and metastasis of tumor cells and was one of the major causes of carcinogenesis. Moreover, it had been demonstrated that defective tumor-induced apoptosis significantly raised the threshold of tumor cell death, thereby nullifying the cytotoxic effects of conventional chemotherapy and radiotherapy and mediating chemoresistance (Schimmer, 2004). We found that the expression of Bcl-2 was higher in drug-resistant osteosarcoma cells than in drug-sensitive osteosarcoma cells after treated with doxorubicin, whereas the expression of pro-apoptotic proteins was the opposite, leading to defective apoptosis in drug-resistant osteosarcoma cells, inhibiting apoptosis and mediating doxorubicin chemoresistance. However, compared with drug-resistant osteosarcoma cells, overexpression of miR-506-3p or silencing of STAT3 decreased the expression of Bcl-2 and increased the expression of Bax, which in turn led to a decrease in the Bcl-2/Bax ratio. This result reversed the dysregulation of apoptosis in drug-resistant osteosarcoma cells and promoted apoptosis, thereby improving the sensitivity of drug-resistant osteosarcoma cells to doxorubicin.

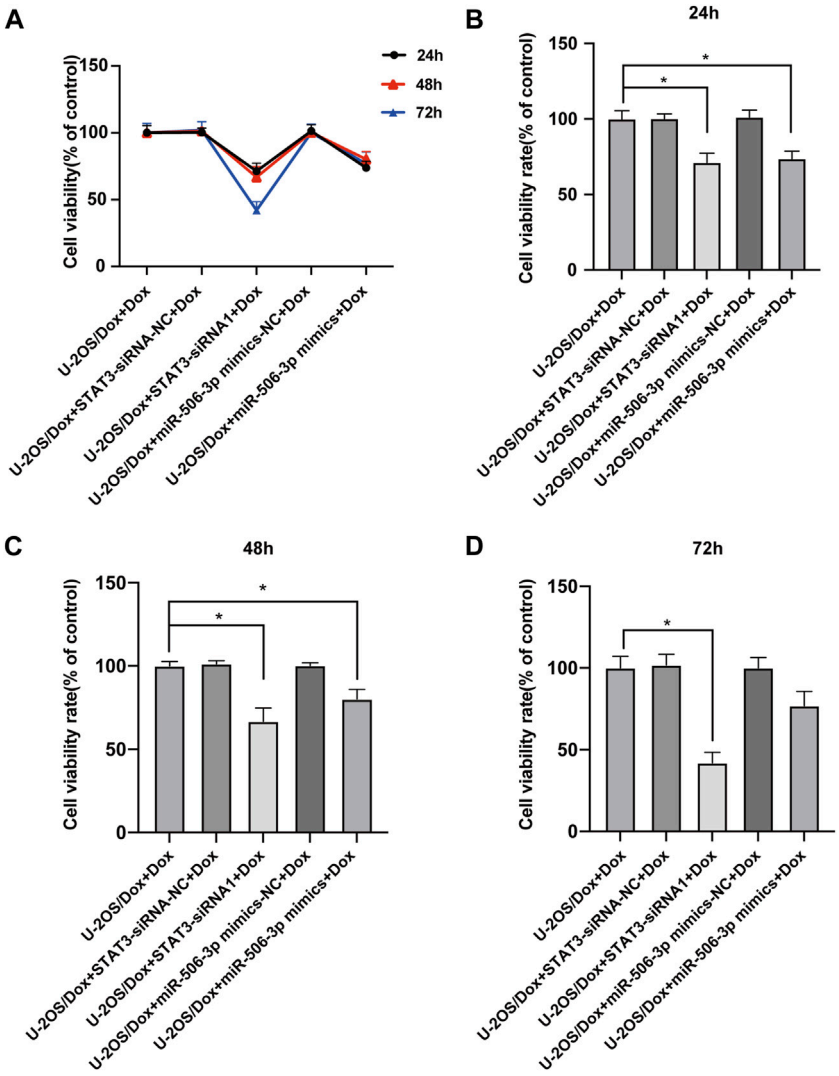

FIGURE 10
The proliferation abilities of drug-resistant osteosarcoma cells were both inhibited by miR-506-3p overexpression and silencing STAT3 **(A)** U-2OS/Dox cells were divided into 5 groups for different treatments, the cell proliferation abilities were detected using CCK8 assay after co-cultured with 29 μg/mL doxorubicin for 24 h, 48 h and 72 h **(B–D)** The cell proliferation activities of the overexpression of miR-506-3p group and the silencing of STAT3 group were both significantly reduced, compared with the U-2OS/Dox + Dox group. *: $p < 0.05$, **: $p < 0.01$.

Moreover, it had been found that Survivin expression was elevated in tumor tissues of chemotherapy-resistant osteosarcoma patients, and that continued chemotherapy could mediate the enrichment of high Survivin-expressing osteosarcoma cells, which ultimately lead to the development of multidrug resistance in the clinic (Wei et al., 2021). As an important downstream effector, downregulation of Survivin expression significantly reduces the incidence of chemoresistance development in osteosarcoma (Tsai et al., 2014). Our study also confirmed that Survivin was highly expressed in osteosarcoma-resistant cells, and overexpression of miR-506-3p or silencing of STAT3 was able to inhibit Survivin expression, thereby enhancing the sensitivity of drug-resistant osteosarcoma cells to doxorubicin.

The higher degree of drug accumulation in tumor cells, the stronger ability to kill tumor cells. The efficacy of doxorubicin, a substrate of p-glycoprotein (P-gP), is influenced by the active efflux of the drug mediated by the ATP-binding cassette (ABC) transporter protein. The efflux effect led to a decrease in intracellular doxorubicin concentration and the development of acquired resistance, which given rise to recurrence or deterioration in nearly one-third of osteosarcoma patients (Kathawala et al., 2015). It had been demonstrated that inhibition of MDR1/ABCB1 or MRP1/ABCC1 in the ABC transporter protein family could reverse doxorubicin resistance in tumor cells including osteosarcoma (Tsang et al., 2003; Sampson et al., 2019; Gerardo-Ramirez et al., 2022; Packeiser et al., 2023). The results of the present study showed that the expression levels of both MDR1/ABCB1 and MRP1/ABCC1 in drug-resistant osteosarcoma cells line U-2OS/Dox were significantly higher than those in drug-sensitive osteosarcoma cells line U-2OS. The enhanced action of these membrane efflux pumps led to a decrease in the concentration of antitumor drugs in osteosarcoma cells, thus, acquired resistance occurred (Gonzalez-Fernandez et al., 2017). However, decreasing the expression levels of MDR1/ABCB1 and MRP1/ABCC1 in U-2OS/Dox increased the chemosensitivity of drug-resistant osteosarcoma cells to doxorubicin.

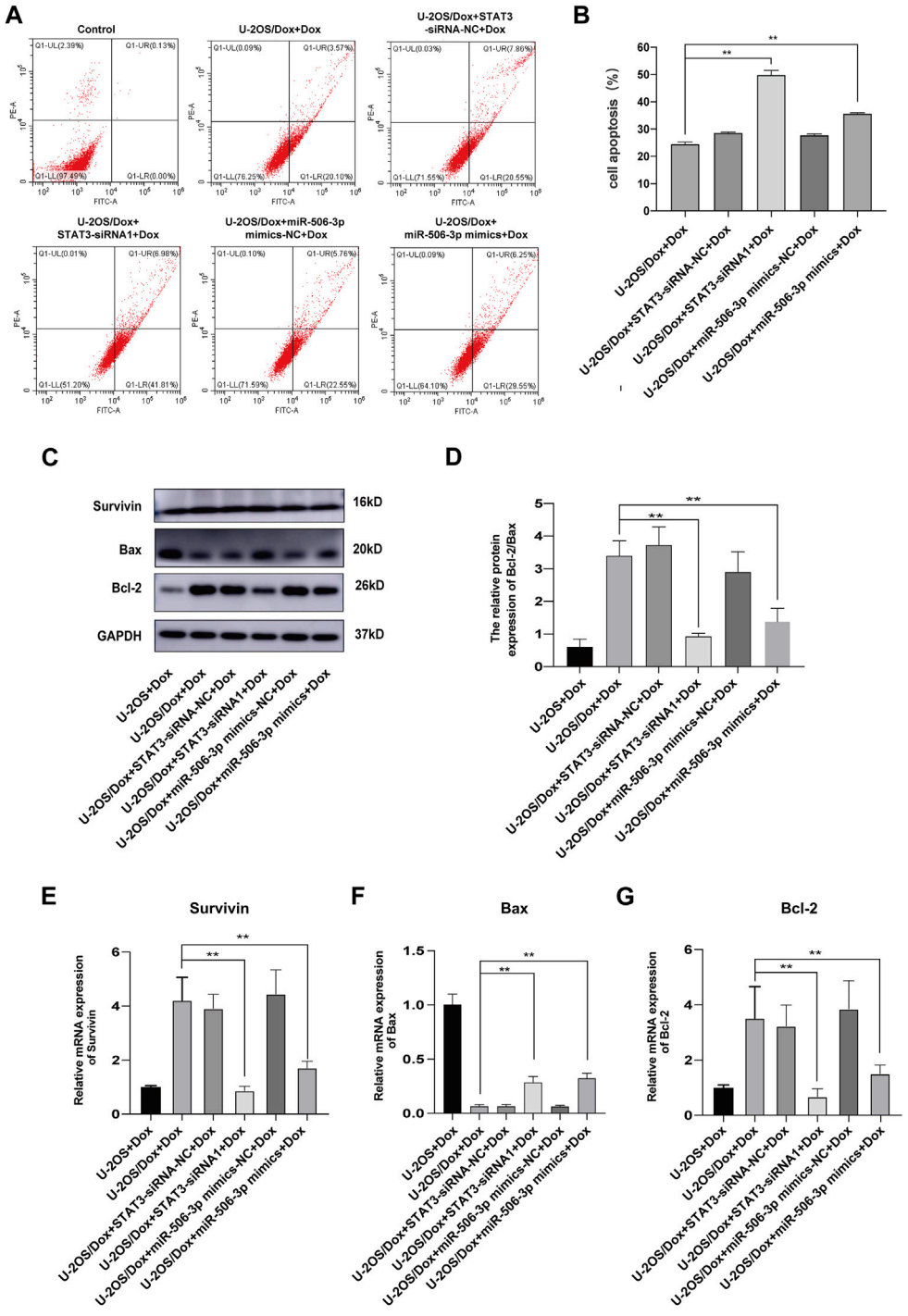

FIGURE 11
The apoptosis of drug-resistant osteosarcoma cells was both increased by miR-506-3p overexpression and silencing STAT3 **(A, B)** The apoptosis rate of each group was detected using Annexin V-FITC/PI double-stained apoptosis cassette. The apoptosis rates were both significantly higher in the overexpression of miR-506-3p group and the silencing of STAT3 group by flow cytometry. **(C)** The Western blot protein bands of Survivin, Bax and Bcl-2. **(D)** The relative protein expression ratio of Bcl-2/Bax was significantly reduced in the overexpression of miR-506-3p group and the silencing STAT3 group by Western blot. The mRNA expressions of the apoptotic proteins Survivin **(E)** and Bcl-2 **(G)** were both inhibited by overexpression of miR-506-3p and silencing of STAT3 through RT-qPCR, and the mRNA expression level of Bax **(F)** was significantly increased. **: $p < 0.01$.

JAK2 was a tyrosine kinase that existed under the cell membrane, and it could bind to various cytokine receptors to activate transcription factors such as STAT3 (Huang et al., 2022), an intranuclear transcription factor that promotes cell proliferation, differentiation, apoptosis, and immune response (Ma et al., 2020). Under normal physiological conditions, the JAK2/STAT3 signaling pathway was involved in many important biological processes, such as embryonic development, immune response, cell proliferation and differentiation. However, under certain pathological conditions, the JAK2/STAT3 signaling pathway was also abnormally activated, cytokines

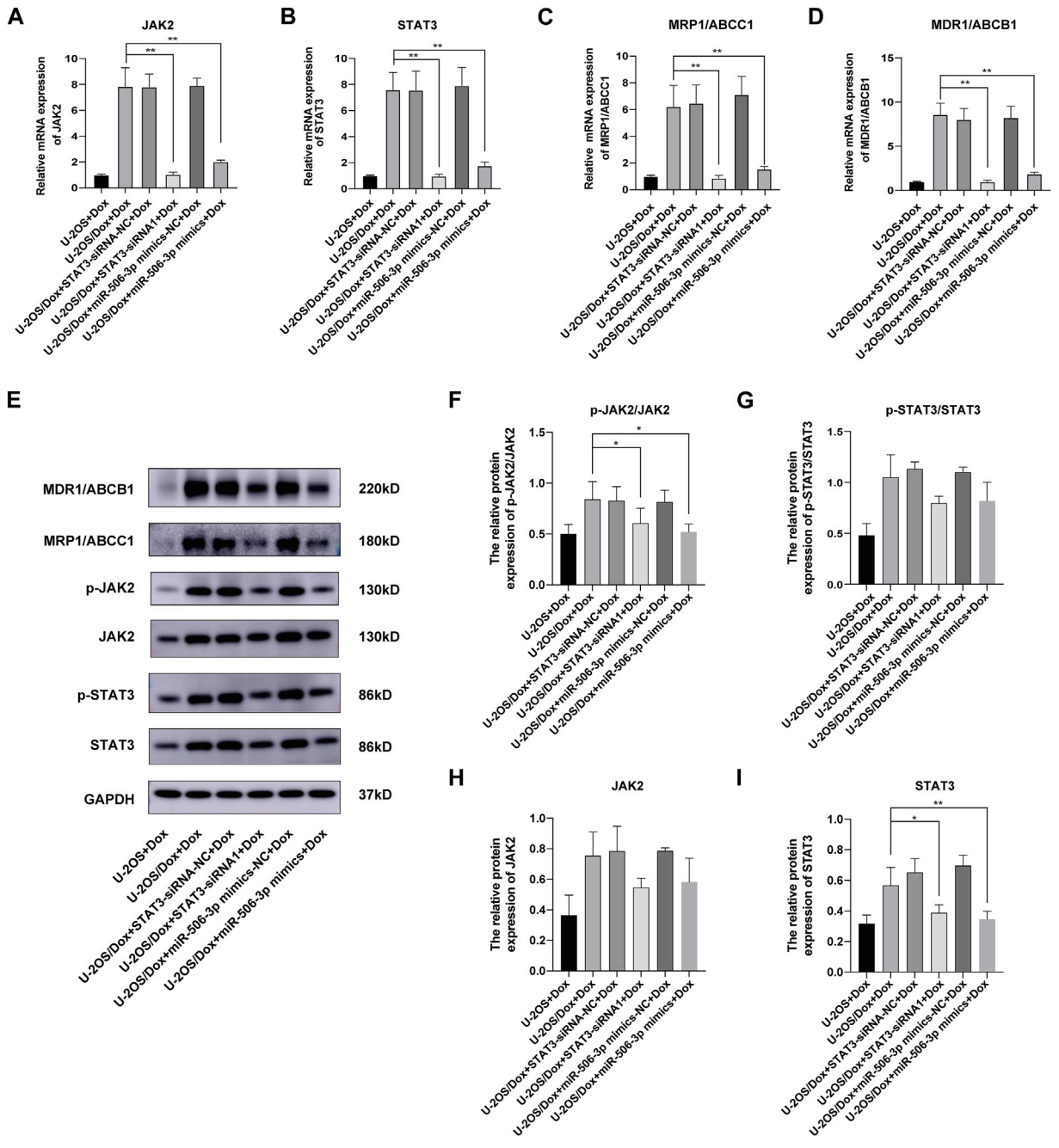

FIGURE 12
Overexpression of miR-506-3p and silencing STAT3 could both inhibit the expression of drug-resistant proteins in drug-resistant osteosarcoma cells by targeting the JAK2-STAT3 signaling pathway The mRNA expressions of JAK2 **(A)**, STAT3 **(B)**, MRP1/ABCC1 **(C)** and MDR1/ABCB1 **(D)** were both inhibited by miR-506-3p overexpression and silencing STAT3, compared with the U-2OS/Dox + Dox group. **(E)** The Western blot protein bands of STAT3, p-STAT3, JAK2, p-JAK2, MRP1/ABCC1 and MDR1/ABCB1. Densitometry analysis for p-JAK2/JAK2 **(F)**, p-STAT3/STAT3 **(G)**, JAK2 **(H)** and STAT3 **(I)**, showed that protein expression levels of p-JAK2/JAK2 and STAT3 were significantly reduced. *: $p < 0.05$, **: $p < 0.01$.

bind to their corresponding receptors, leading to recruitment of related JAKs, further change to p-JAK, JAK activation leads to formation of docking sites for STAT, STATs are phosphorylated to p-STAT by tyrosine, STATs dissociate from the receptor to form dimers, STAT dimers enter the nucleus, bind to DNA, and regulate transcription, the JAK/STAT signaling pathway is activated (Hu et al., 2021; Wang et al., 2022). Our study found that overexpression of miR-506-3p and silencing STAT3 inhibited the mRNA expression levels of JAK2 and STAT3 genes. However, at the protein expression level, overexpression of miR-506-3p and silencing of STAT3 expression had a significant inhibitory effect on the expression of p-JAK2/JAK2 and STAT3 total proteins, and there were no statistically significant differences on the expression of p-STAT3/STAT3 and JAK2 total proteins. It suggested that miR-506-3p might be able to reverse chemoresistance to doxorubicin in drug-resistant osteosarcoma cells by inhibiting the phosphorylation of JAK2 and the expression of total STAT3 protein in

drug-resistant osteosarcoma cells and inhibiting the over-activation of JAK2/STAT3 signaling pathway. Of course, the specific mechanism of miR-506-3p in the regulation of JAK2/STAT3 signaling pathway in Doxorubicin-resistant osteosarcoma patients needs to be further investigated.

4 Conclusion

In summary, the study demonstrated that miR-506-3p could inhibit JAK2/STAT3 signaling pathway by directly binding STAT3, thus reversed the malignant biological behaviors such as proliferation, migration and invasion of drug-resistant osteosarcoma cells, promoted cell apoptosis, as well as inhibited the expressions of drug-resistant proteins. Our study provided theoretical support for improving chemical sensitivity of drug-resistant osteosarcoma cells in an attempt to solve the problem of doxorubicin resistance in osteosarcoma treatment.

5 Materials and methods

5.1 Construction and cell culture of drug-resistant osteosarcoma cell line U-2OS/Dox

The human osteosarcoma cell line U-2OS was obtained from the Chinese Academy of Sciences (Shanghai, China). The doxorubicin-resistant cell line U-2OS/Dox was measured using an intermittent stepwise increase method (Serra et al., 1993). U-2OS cells in logarithmic phase were taken, and doxorubicin was used as the inducing drug, and drug resistance of U-2OS cells was induced by gradually increasing the drug concentration of doxorubicin (30 ng/mL, 100 ng/mL and 580 ng/mL), and each concentration was shocked for 9 times, and then after the cells grew stably in this concentration, the concentration of the drug was increased to continue the culture. Doxorubicin drug induction lasted 6–8 months until the cells were able to grow stably in 580 ng/mL doxorubicin. The IC_{50} of the resistant cell lines was detected and the RI was calculated. RI = [IC_{50} of the resistant cell line]/[IC_{50} of the parental cell line], and RI > 10 was considered that the resistant cell line met the requirements. Both cell lines were cultured in McCoys (GIBCO, Invitrogen, Carlsbad, CA, United States) supplemented with 10% fetal bovine serum (GIBCO, Invitrogen, Carlsbad, CA, United States) in a constant temperature incubator at 37°C with 5% CO_2.

5.2 Bioinformatics predictions

TargetScan Human 8.0 (https://www.targetscan.org/vert_80 (McGeary et al., 2019) was used to predict biological targets of miR-506-3p by searching for the presence of conserved 8mer, 7mer, and 6mer sites that match the seed region of each miRNA. Tumor-miRNA-Pathway (http://bioinfo.life.hust.edu.cn/miR_path/index.html) (Ma et al., 2016), miRWalk (http://mirwalk.umm.uni-heidelberg.de/) (Sticht et al., 2018) and miRDB (https://mirdb.org/) (Chen and Wang, 2020) were used to predict the target genes of miR-506-3p. Then the intersection of three databases was taken. We also searched the expression profiles of miR-506-3p in different tumor tissues and their paracancerous tissues using the Tumor-miRNA-Pathway database. After that, GO and KEGG enrichment analysis of the screened miR-506-3p target genes was performed using the DAVID database (https://david.ncifcrf.gov/home.jsp) (Jiao et al., 2012). Finally, PPI networks were constructed, including physical and functional associations, for the selected miR-506-3p target genes using the STRING database (https://cn.string-db.org/) (Szklarczyk et al., 2021). We selected the default parameter of the system, a medium confidence of 0.400, to screen 30 interacting target genes. In addition, the hub target genes were explored using the cytoHubba plug-in and degree topology algorithm in Cytoscape (version 3.8.0) software.

5.3 Dual luciferase reporter gene assay

The 293T cells and target plasmids were prepared for transfection beforehand, when the cell density reached 50%–70%. Solution A was prepared by combining 10 μL DMEM, 0.16 μg of h-STAT3-3′-UTR target plasmid and 5 p.m. of hsa-miR-506-3p NC at room temperature. Solution B was prepared by combining 10 μL DMEM with 0.3 μL transfection reagent (Hanhen Bio-products LipoFiter™, the concentration of which is 0.8 mg/mL) and left at room temperature for 5 min. Solution A and solution B were thoroughly mixed and left for 20 min. After 6 h of transfection, fresh medium was changed, and the cells were collected after 48 h of transfection, and the luciferase activity was detected by fluorescence detector.

5.4 Cell transfection

U-2OS cells and U-2OS/Dox cells were used as transfection targets in logarithmic growth phase. Cells were inoculated in 6-well plates 24 h prior to transfection, and transfection was carried out when the cell confluence was about 50%, and the cell culture medium was changed 30 min prior to transfection, with reference to the instructions of the transfection reagent of lipofectamine 3000 (thermo, L3000001, United States). The cells were first respectively transfected into U-2OS/Dox cells with STAT3-siRNA1, siRNA2, siRNA3 and siRNA-NC (Ribobio, Guangzhou, China) at the final concentration of 50 nM, which were targeted to the STAT3 mRNA and screened for the best STAT3-siRNA. MiR-506-3p mimics and miR-506-3p mimics-NC (Hanheng, Shanghai, China) were transfected into U-2OS/Dox cells at a final concentration of 50 nM, and cells were harvested 48 h after transfection. The primers of STAT3-siRNA1, siRNA2, siRNA3, miR-506-3p mimics and miR-506-3p mimics-NC were 5′-GGCGTC CAGTTCACTACTA-3′, 5′-AGACCCGTCAACAAATTAA-3′, 5′-CATCGAGCAGCTGACTACA-3′, 5′-UAAGGCACCCUUCUGAGU AGA-3′ and 5′-UCACAACCUCCUCCUGAGUAGA-3′, respectively.

5.5 CCK8 assay

5.5.1 CCK8 detection of U-2OS and U-2OS/Dox cell viability

U-2OS and U-2OS/Dox cells were inoculated into 96-well plates at 6×10^3/well for 24 h. Increasing concentrations of doxorubicin (0, 0.5, 1, 2, 4, 8, 16, 32 μg/mL) were added to the plates and blank control wells without cytosol were set up, with

three replicate wells for each treatment. After 24 h of incubation, 10 μL CCK8 reagent (Kemix, Beijing, China) was added to each well, and the absorbance at 450 nm was measured on an enzyme labeler after another 1.5 h of incubation (A). Cell viability (%) = [A (experiment)—A (blank)]/[A (control)—A (blank)] × 100%. The IC_{50} values of U-2OS and U-2OS/Dox cells were determined by plotting the concentration-effect histogram with the drug concentration as the horizontal coordinate and the cell survival rate as the vertical coordinate.

5.5.2 CCK8 detection of U-2OS/Dox cell viability after transfection with miR-506-3p mimics

The cells were divided into five groups: blank control group (U-2OS/Dox group), negative control group (U-2OS/Dox + STAT3-siRNA-NC group, U-2OS/Dox + miR-506-3p mimics-NC group) and experimental group (U-2OS/Dox + STAT3-siRNA1 group, U-2OS/Dox + miR-506-3p mimics group). The group-treated cells in step 5.4 were inoculated into 96-well plates and pre-cultured for 24 h, 48 h and 72 h. Then 10 μL CCK8 reagents was added, and then the absorbance at 450 nm wavelength was measured on the enzyme labeling instrument after incubation for another 1.5 h. The absorbance at 450 nm wavelength was determined (A). Cell viability (%) = [A (experiment)—A (blank)]/[A (control)—A (blank)] × 100%. The difference in cell viability of U-2OS/Dox cells transfected with miR-506-3p mimics was analyzed and compared with that of U-2OS/Dox cells of the original drug-resistant strain.

5.6 RT-qPCR assay

The cells were divided into 6 groups: U-2OS group, blank control group (U-2OS/Dox group), negative control group (U-2OS/Dox + STAT3-siRNA-NC group, U-2OS/Dox + miR-506-3p mimics-NC group) and experimental group (U-2OS/Dox + STAT3-siRNA1 group, U-2OS/Dox + miR-506-3p mimics group).The cells in logarithmic growth phase were taken and the total RNA in the cells was extracted using Trizol reagent total RNA extraction kit (Vazyme, Nanjing, China). MiRNA and mRNA were reverse transcribed into cDNA according to the procedure of Reverse Transcription Kit (Takara, Japan), the reaction was terminated after incubation at 50°C for 15 min and at 75°C for 5 min, and then subjected to real-time fluorescence quantitative analysis. The mRNA fluorescence quantification was performed by dye method, and the final concentration of both forward primer and reverse primer was 50 nM. Predegeneration was 95°C for 5 min, and amplification was performed at 95°C for 10 s, 60°C for 10 s, and 72°C for 10 s, a total of 40 cycles. The solubility curves were plotted and analysed based on $2^{-\Delta\Delta ct}$ calculations. All genes and their corresponding specific primer sequences (5′-3′) were shown in Table 1.

TABLE 1 The primers of genes used for RT-qPCR.

Gene name	Direction	Sequence
STAT3	Forward	AGCAGCACCTTCAGGATGTC
	Reverse	GCATCTTCTGCCTGGTCACT
JAK2	Forward	TGGAGGGAACATCCACCTCT
	Reverse	TCTGCCTCAGATTTCCCAAGG
miR-506-3p	Forward	ACCACCGTAAGGCACCCTTCT
	Reverse	ATCCAGTGCAGGGTCCGAGG
MDR1/ABCB1	Forward	GCTGTCAAGGAAGCCAATGC
	Reverse	GAGGATCTTGGGGTTGCGAA
MRP1/ABCC1	Forward	TCCCCTGAACATTCTCCCCA
	Reverse	ATGCTGTCAGGTTCCAGCTC
Survivin	Forward	GAGGCTGGCTTCATCCACT
	Reverse	TGGTTTCCTTTGCATGGGGT
Bax	Forward	CCCCCGAGAGGTCTTTTTCC
	Reverse	CTGATCAGTTCCGGCACCTT
Bcl-2	Forward	TGGTGGAGGAGCTCTTCAGG
	Reverse	CTCTCCACACACATGACCCC
GAPDH	Forward	ATTCCACCCATGGCAAATTCC
	Reverse	GACTCCACGACGTACTCAGC
U6 (by stem-loop)	Forward	AGAGAAGATTAGCATGGCCCCTG
	Reverse	CAGTGCAGGGTCCGAGGT

5.7 Western blot assay

The cells were centrifuged at 2500 rpm for 5 min, then protein cleavaged with strong RIPA lysis buffer (CWBIO, Jiangsu, China), and centrifuged at 13,000 rpm for 6 min at 4°C to collect the total proteins, and the protein concentration was measured by BCA kit. After denaturation at 98°C for 10 min, the proteins were separated by 10% SDS-PAGE and transferred onto a PVDF membrane. The membrane was incubated with primary antibody at 4°C overnight, rinsed, and then incubated with secondary antibody at room temperature for 2 h. Finally, enhanced chemiluminescence (ECL) reaction was performed and visualized, and the images were processed using ImageJ software to calculate the relative protein expression levels. Primary antibodies were anti-STAT3 (1:1000, #30835, CST, Danvers, MA, United States), anti-p-STAT3 (1:1000, #94994, CST), anti-JAK2 (1:1000, YT2426, ImmunoWay, United States), anti-p-JAK2 (1:1000, YP0306, ImmunoWay), anti-MDR1/ABCB1 (1:1000, #13342, CST), anti-MRP1/ABCC1 (1:1000, #14685, CST), anti-Survivin (1:1000, #2808, CST), anti-Bax (1:1000, #2772, CST), anti-Bcl-2 (1:1000, #3498, CST), and anti-β-actin (1:1000, #8457, CST), anti-GAPDH (1:10000, AP0063, Bioworld, United States). Secondary antibodies were HPR-conjugated goat anti-mouse (1:10000, abs20039, absin, Shanghai, China), goat anti-rabbit (1:10000, abs20040, absin), and goat anti-rabbit (1:10000, E030120-01, Earthox, United States).

5.8 Cell mobility scratch assay

The cells of each group were inoculated in 6-well plates at a density of 2×10^5/well, and transfection was carried out when the cell density reached 50%. After the cells were spread all over the bottom of the plate,

the cells were gently scratched vertically with the tip of a 200 μL pipette and rinsed gently with PBS for 2 times, and then cultured in low-serum medium (containing 2% FBS) for 24 h. The cellular healing images of the scratches were observed and photographed under a microscope at the moment of scratches (0 h), 24 h and 48 h, and the widths of the scratches were measured to calculate the cell migration force. Cell migration force = [scratch width (0 h)—scratch width (24 h or 48 h)]/scratch width (0 h) × 100%.

5.9 Transwell assay for cell invasiveness

Two hundreds microliter of cell suspension for each group (5×10^4 cells) were added to the Transwell coated with Matrigel matrix gel, and 600 μL complete culture medium containing 10% FBS was added to the lower chamber. After incubation for 24 h, the non-migrated cells were wiped off from the membrane of the upper chamber, and the membrane of the lower chamber was fixed with 4% paraformaldehyde for 10 min. After drying naturally, the membrane was stained with 0.5% crystalline violet solution for 15 min at room temperature, and then observed under an inverted microscope. Three 100 × fields of view were randomly taken for photographing, and the total number of cells in the five different fields of view (top, bottom, left, right and center) were counted and averaged to calculate the cell migration rate.

5.10 Flow cytometry

Cells were digested with EDTA-free trypsin, and the density of each cell suspension was adjusted to 2×10^5 cells/mL. One millilitre of cell suspension was added into a sterile centrifuge tube, and the cells were centrifuged at 2000 rpm for 5 min at room temperature to collect the cells, and the supernate was discarded. The cells were washed twice with pre-cooled PBS (4°C), and 300 μL 1× binding buffer was added to resuspend the cells. Cells were washed twice with pre-cooled PBS (4°C), resuspended by adding 300 μL 1× binding buffer. According to the instructions of the Annexin V-FITC/PI Dual Staining Apoptosis Detection Kit (BD Biosciences, 556547, United States), incubated for 15 min at room temperature with 5 μL Annexin V-FITC, and then 5 μL PI was added for 5 min prior to the start-up of the detection. The apoptosis rate of each group was detected by flow cytometry, and the total apoptosis rate (%) = [early apoptosis rate (Q4 quadrant percentage)] + [late apoptosis rate (Q2 quadrant percentage)].

5.11 Statistical analysis

Data were obtained from at least three independent replicated experiments and the results were expressed as mean ± standard deviation ($\bar{x} \pm s$). Data were analyzed and processed using IBM SPSS 24.0 and GraphPad Prism 9.0.0 software. Comparisons between multiple groups were analyzed by one-way ANOVA or Kruskal-Walis H Test, and comparisons between two groups were made by *t*-Test or Mann-Whitney *U* Test, with $p < 0.05$ indicating that the differences were statistically significant.

Data availability statement

The original contributions presented in the study are included in the article/Supplementary Material, further inquiries can be directed to the corresponding authors.

Author contributions

XW: Funding acquisition, Supervision, Writing–original draft. RD: Investigation, Methodology, Writing–original draft. ZF: Formal Analysis, Methodology, Writing–original draft. MY: Formal Analysis, Methodology, Writing–original draft. DL: Writing–review and editing, Project administration. YZ: Writing–review and editing, Funding acquisition, Project administration. CQ: Conceptualization, Writing–review and editing. WZ: Visualization, Writing–original draft. LS: Investigation, Methodology, Writing–review and editing. JZ: Funding acquisition, Supervision, Writing–original draft. YC: Conceptualization, Funding acquisition, Validation, Writing–review and editing.

Funding

The author(s) declare financial support was received for the research, authorship, and/or publication of this article. This research work was supported by the Joint Co-construction Project of Medical Science and Technology Research Plan of Henan Province (No. LHGJ20200286), the Key Scientific and Technology Project of Henan Province (No. 222102310358) and the Young Teacher Fostering Foundation of Zhengzhou University (Nos JC23862096 and JC21854039).

Conflict of interest

The authors declare that the research was conducted in the absence of any commercial or financial relationships that could be construed as a potential conflict of interest.

Publisher's note

Supplementary material

The Supplementary Material for this article can be found online at: https://www.frontiersin.org/articles/10.3389/fphar.2024.1303732/full#supplementary-material

References

Barre, B., Vigneron, A., Perkins, N., Roninson, I. B., Gamelin, E., and Coqueret, O. (2007). The STAT3 oncogene as a predictive marker of drug resistance. *Trends Mol. Med.* 13 (1), 4–11. doi:10.1016/j.molmed.2006.11.001

Barton, B. E. (2006). STAT3: a potential therapeutic target in dendritic cells for the induction of transplant tolerance. *Expert Opin. Ther. Targets* 10 (3), 459–470. doi:10.1517/14728222.10.3.459

Chen, Y., and Wang, X. (2020). miRDB: an online database for prediction of functional microRNA targets. *Nucleic Acids Res.* 48 (D1), D127–D131. doi:10.1093/nar/gkz757

Chen, Y., Zhu, Y., Sheng, Y., Xiao, J., Xiao, Y., Cheng, N., et al. (2019). SIRT1 downregulated FGB expression to inhibit RCC tumorigenesis by destabilizing STAT3. *Exp. Cell Res.* 382 (2), 111466. doi:10.1016/j.yexcr.2019.06.011

Chou, A. J., and Gorlick, R. (2006). Chemotherapy resistance in osteosarcoma: current challenges and future directions. *Expert Rev. Anticancer Ther.* 6 (7), 1075–1085. doi:10.1586/14737140.6.7.1075

Cong, C., Wang, W., Tian, J., Gao, T., Zheng, W., and Zhou, C. (2018). Identification of serum miR-124 as a biomarker for diagnosis and prognosis in osteosarcoma. *Cancer Biomark.* 21 (2), 449–454. doi:10.3233/CBM-170672

Dong, L., Qu, F., and Qu, F. (2020). CircUBAP2 promotes SEMA6D expression to enhance the cisplatin resistance in osteosarcoma through sponging miR-506-3p by activating Wnt/β-catenin signaling pathway. *J. Mol. Histol.* 51 (4), 329–340. doi:10.1007/s10735-020-09883-8

Elfadadny, A., El-Husseiny, H. M., Abugomaa, A., Ragab, R. F., Mady, E. A., Aboubakr, M., et al. (2021). Role of multidrug resistance-associated proteins in cancer therapeutics: past, present, and future perspectives. *Environ. Sci. Pollut. Res. Int.* 28 (36), 49447–49466. doi:10.1007/s11356-021-15759-5

Fu, H., Wu, Y., Chen, J., Hu, X., Wang, X., and Xu, G. (2023). Exosomes and osteosarcoma drug resistance. *Front. Oncol.* 13, 1133726. doi:10.3389/fonc.2023.1133726

Gerardo-Ramirez, M., Keggenhoff, F. L., Giam, V., Becker, D., Groth, M., Hartmann, N., et al. (2022). CD44 contributes to the regulation of MDR1 protein and doxorubicin chemoresistance in osteosarcoma. *Int. J. Mol. Sci.* 23 (15), 8616. doi:10.3390/ijms23158616

Gonzalez-Fernandez, Y., Imbuluzqueta, E., Zalacain, M., Mollinedo, F., Patino-Garcia, A., and Blanco-Prieto, M. J. (2017). Doxorubicin and edelfosine lipid nanoparticles are effective acting synergistically against drug-resistant osteosarcoma cancer cells. *Cancer Lett.* 388, 262–268. doi:10.1016/j.canlet.2016.12.012

Hattinger, C. M., Fanelli, M., Tavanti, E., Vella, S., Ferrari, S., Picci, P., et al. (2015). Advances in emerging drugs for osteosarcoma. *Expert Opin. Emerg. Drugs* 20 (3), 495–514. doi:10.1517/14728214.2015.1051965

Hu, F. Y., Cao, X. N., Xu, Q. Z., Deng, Y., Lai, S. Y., Ma, J., et al. (2016). miR-124 modulates gefitinib resistance through SNAI2 and STAT3 in non-small cell lung cancer. *J. Huazhong Univ. Sci. Technol. Med. Sci.* 36 (6), 839–845. doi:10.1007/s11596-016-1672-x

Hu, M., Yuan, X., Liu, Y., Tang, S., Miao, J., Zhou, Q., et al. (2017). IL-1β-induced NF-κB activation down-regulates miR-506 expression to promotes osteosarcoma cell growth through JAG1. *Biomed. Pharmacother.* 95, 1147–1155. doi:10.1016/j.biopha.2017.08.120

Hu, X., Li, J., Fu, M., Zhao, X., and Wang, W. (2021). The JAK/STAT signaling pathway: from bench to clinic. *Signal Transduct. Target Ther.* 6 (1), 402. doi:10.1038/s41392-021-00791-1

Hu, Y. S., Han, X., and Liu, X. H. (2019). STAT3: a potential drug target for tumor and inflammation. *Curr. Top. Med. Chem.* 19 (15), 1305–1317. doi:10.2174/1568026619666190620145052

Hu, Z., Fan, H., Lv, G., Zhou, Q., Yang, B., Zheng, J., et al. (2015). 5-Aminolevulinic acid-mediated sonodynamic therapy induces anti-tumor effects in malignant melanoma via p53-miR-34a-Sirt1 axis. *J. Dermatol Sci.* 79 (2), 155–162. doi:10.1016/j.jdermsci.2015.04.010

Hu, Z., Wen, S., Huo, Z., Wang, Q., Zhao, J., Wang, Z., et al. (2022). Current status and prospects of targeted therapy for osteosarcoma. *Cells* 11 (21), 3507. doi:10.3390/cells11213507

Huang, B., Lang, X., and Li, X. (2022). The role of IL-6/JAK2/STAT3 signaling pathway in cancers. *Front. Oncol.* 12, 1023177. doi:10.3389/fonc.2022.1023177

Jia, F., Liu, Y., Dou, X., Du, C., Mao, T., and Liu, X. (2022). Liensinine inhibits osteosarcoma growth by ROS-mediated suppression of the JAK2/STAT3 signaling pathway. *Oxid. Med. Cell Longev.* 2022, 8245614. doi:10.1155/2022/8245614

Jiao, X., Sherman, B. T., Huang da, W., Stephens, R., Baseler, M. W., Lane, H. C., et al. (2012). DAVID-WS: a stateful web service to facilitate gene/protein list analysis. *Bioinformatics* 28 (13), 1805–1806. doi:10.1093/bioinformatics/bts251

Jiashi, W., Chuang, Q., Zhenjun, Z., Guangbin, W., Bin, L., and Ming, H. (2018). MicroRNA-506-3p inhibits osteosarcoma cell proliferation and metastasis by suppressing RAB3D expression. *Aging (Albany NY)* 10 (6), 1294–1305. doi:10.18632/aging.101468

Kathawala, R. J., Gupta, P., Ashby, C. R., Jr., and Chen, Z. S. (2015). The modulation of ABC transporter-mediated multidrug resistance in cancer: a review of the past decade. *Drug Resist Updat* 18, 1–17. doi:10.1016/j.drup.2014.11.002

Li, C., Lin, X., Zhang, C., Wan, L., Yin, J., and Wang, B. (2021). Long non-coding RNA FGD5-AS1 enhances osteosarcoma cell proliferation and migration by targeting miR-506-3p/RAB3D axis. *Hum. Cell* 34 (4), 1255–1265. doi:10.1007/s13577-021-00536-w

Li, L., Wei, H., Zhang, H., Xu, F., and Che, G. (2020). Circ_100565 promotes proliferation, migration and invasion in non-small cell lung cancer through upregulating HMGA2 via sponging miR-506-3p. *Cancer Cell Int.* 20, 160. doi:10.1186/s12935-020-01241-8

Li, X., and Liu, J. (2023). FANCD2 inhibits ferroptosis by regulating the JAK2/STAT3 pathway in osteosarcoma. *BMC Cancer* 23 (1), 179. doi:10.1186/s12885-023-10626-7

Lilienthal, I., and Herold, N. (2020). Targeting molecular mechanisms underlying treatment efficacy and resistance in osteosarcoma: a review of current and future strategies. *Int. J. Mol. Sci.* 21 (18), 6885. doi:10.3390/ijms21186885

Liu, C., Xing, H., Guo, C., Yang, Z., Wang, Y., and Wang, Y. (2019). MiR-124 reversed the doxorubicin resistance of breast cancer stem cells through STAT3/HIF-1 signaling pathways. *Cell Cycle* 18 (18), 2215–2227. doi:10.1080/15384101.2019.1638182

Liu, Y., Liao, S., Bennett, S., Tang, H., Song, D., Wood, D., et al. (2021). STAT3 and its targeting inhibitors in osteosarcoma. *Cell Prolif.* 54 (2), e12974. doi:10.1111/cpr.12974

Liu, Y., Yan, W., Zhou, D., Jin, G., and Cheng, X. (2020). Long non-coding RNA HOXA11-AS accelerates cell proliferation and epithelial-mesenchymal transition in hepatocellular carcinoma by modulating the miR-506-3p/Slug axis. *Int. J. Mol. Med.* 46 (5), 1805–1815. doi:10.3892/ijmm.2020.4715

Lossi, L. (2022). The concept of intrinsic versus extrinsic apoptosis. *Biochem. J.* 479 (3), 357–384. doi:10.1042/BCJ20210854

Lu, M., Xie, K., Lu, X., Lu, L., Shi, Y., and Tang, Y. (2021). Notoginsenoside R1 counteracts mesenchymal stem cell-evoked oncogenesis and doxorubicin resistance in osteosarcoma cells by blocking IL-6 secretion-induced JAK2/STAT3 signaling. *Invest. New Drugs* 39 (2), 416–425. doi:10.1007/s10637-020-01027-9

Ma, J. H., Qin, L., and Li, X. (2020). Role of STAT3 signaling pathway in breast cancer. *Cell Commun. Signal.* 18 (1), 33. doi:10.1186/s12964-020-0527-z

Ma, X., Xu, W., Jin, X., Mu, H., Wang, Z., Hua, Y., et al. (2023). Telocinobufagin inhibits osteosarcoma growth and metastasis by inhibiting the JAK2/STAT3 signaling pathway. *Eur. J. Pharmacol.* 942, 175529. doi:10.1016/j.ejphar.2023.175529

Ma, Z., Liu, T., Huang, W., Liu, H., Zhang, H. M., Li, Q., et al. (2016). MicroRNA regulatory pathway analysis identifies miR-142-5p as a negative regulator of TGF-β pathway via targeting SMAD3. *Oncotarget* 7 (44), 71504–71513. doi:10.18632/oncotarget.12229

McGeary, S. E., Lin, K. S., Shi, C. Y., Pham, T. M., Bisaria, N., Kelley, G. M., et al. (2019). The biochemical basis of microRNA targeting efficacy. *Science* 366(6472), eaav1741. doi:10.1126/science.aav1741

Mengie Ayele, T., Tilahun Muche, Z., Behaile Teklemariam, A., Bogale Kassie, A., and Chekol Abebe, E. (2022). Role of JAK2/STAT3 signaling pathway in the tumorigenesis, chemotherapy resistance, and treatment of solid tumors: a systemic review. *J. Inflamm. Res.* 15, 1349–1364. doi:10.2147/JIR.S353489

Packeiser, E. M., Engels, L., Nolte, I., Goericke-Pesch, S., and Murua Escobar, H. (2023). MDR1 inhibition reverses doxorubicin-resistance in six doxorubicin-resistant canine prostate and bladder cancer cell lines. *Int. J. Mol. Sci.* 24 (9), 8136. doi:10.3390/ijms24098136

Peng, T., Zhou, L., Zuo, L., and Luan, Y. (2016). MiR-506 functions as a tumor suppressor in glioma by targeting STAT3. *Oncol. Rep.* 35 (2), 1057–1064. doi:10.3892/or.2015.4406

Qi, M. M., Ge, F., Chen, X. J., Tang, C., and Ma, J. (2019). MiR-124 changes the sensitivity of lung cancer cells to cisplatin through targeting STAT3. *Eur. Rev. Med. Pharmacol. Sci.* 23 (12), 5242–5250. doi:10.26355/eurrev_201906_18190

Rah, B., Rather, R. A., Bhat, G. R., Baba, A. B., Mushtaq, I., Farooq, M., et al. (2022). JAK/STAT signaling: molecular targets, therapeutic opportunities, and limitations of targeted inhibitions in solid malignancies. *Front. Pharmacol.* 13, 821344. doi:10.3389/fphar.2022.821344

Salas, S., Jiguet-Jiglaire, C., Campion, L., Bartoli, C., Frassineti, F., Deville, J. L., et al. (2014). Correlation between ERK1 and STAT3 expression and chemoresistance in patients with conventional osteosarcoma. *BMC Cancer* 14, 606. doi:10.1186/1471-2407-14-606

Sampson, A., Peterson, B. G., Tan, K. W., and Iram, S. H. (2019). Doxorubicin as a fluorescent reporter identifies novel MRP1 (ABCC1) inhibitors missed by calcein-based high content screening of anticancer agents. *Biomed. Pharmacother.* 118, 109289. doi:10.1016/j.biopha.2019.109289

Schimmer, A. D. (2004). Inhibitor of apoptosis proteins: translating basic knowledge into clinical practice. *Cancer Res.* 64 (20), 7183–7190. doi:10.1158/0008-5472.CAN-04-1918

Serra, M., Scotlandi, K., Manara, M. C., Maurici, D., Lollini, P. L., De Giovanni, C., et al. (1993). Establishment and characterization of multidrug-resistant human osteosarcoma cell lines. *Anticancer Res.* 13 (2), 323–329.

Sticht, C., De La Torre, C., Parveen, A., and Gretz, N. (2018). miRWalk: an online resource for prediction of microRNA binding sites. *PLoS One* 13 (10), e0206239. doi:10.1371/journal.pone.0206239

Su, Z., Ye, X., and Shang, L. (2019). MiR-506 promotes natural killer cell cytotoxicity against human hepatocellular carcinoma cells by targeting STAT3. *Yonsei Med. J.* 60 (1), 22–29. doi:10.3349/ymj.2019.60.1.22

Szklarczyk, D., Gable, A. L., Nastou, K. C., Lyon, D., Kirsch, R., Pyysalo, S., et al. (2021). The STRING database in 2021: customizable protein-protein networks, and functional characterization of user-uploaded gene/measurement sets. *Nucleic Acids Res.* 49 (D1), D605–D612. doi:10.1093/nar/gkaa1074

Tang, Z., Lu, Y., Chen, Y., Zhang, J., Chen, Z., and Wang, Q. (2021). Research progress of MicroRNA in chemotherapy resistance of osteosarcoma. *Technol. Cancer Res. Treat.* 20, 15330338211034262. doi:10.1177/15330338211034262

Tsai, H. C., Huang, C. Y., Su, H. L., and Tang, C. H. (2014). CTGF increases drug resistance to paclitaxel by upregulating survivin expression in human osteosarcoma cells. *Biochim. Biophys. Acta* 1843 (5), 846–854. doi:10.1016/j.bbamcr.2014.01.007

Tsang, W. P., Chau, S. P., Fung, K. P., Kong, S. K., and Kwok, T. T. (2003). Modulation of multidrug resistance-associated protein 1 (MRP1) by p53 mutant in Saos-2 cells. *Cancer Chemother. Pharmacol.* 51 (2), 161–166. doi:10.1007/s00280-002-0551-2

Wang, L., Kang, F. B., Sun, N., Wang, J., Chen, W., Li, D., et al. (2016). The tumor suppressor miR-124 inhibits cell proliferation and invasion by targeting B7-H3 in osteosarcoma. *Tumour Biol.* 37 (11), 14939–14947. doi:10.1007/s13277-016-5386-2

Wang, L. N., Zhang, Z. T., Wang, L., Wei, H. X., Zhang, T., Zhang, L. M., et al. (2022). TGF-β1/SH2B3 axis regulates anoikis resistance and EMT of lung cancer cells by modulating JAK2/STAT3 and SHP2/Grb2 signaling pathways. *Cell Death Dis.* 13 (5), 472. doi:10.1038/s41419-022-04890-x

Wang, Y., Lei, X., Gao, C., Xue, Y., Li, X., Wang, H., et al. (2019). MiR-506-3p suppresses the proliferation of ovarian cancer cells by negatively regulating the expression of MTMR6. *J. Biosci.* 44 (6), 126. doi:10.1007/s12038-019-9952-9

Wang, Y. C., Zheng, L. H., Ma, B. A., Zhou, Y., Zhang, M. H., Zhang, D. Z., et al. (2011). Clinical value of signal transducers and activators of transcription 3 (STAT3) gene expression in human osteosarcoma. *Acta histochem.* 113 (4), 402–408. doi:10.1016/j.acthis.2010.03.002

Wei, C., Yang, C., Wang, S., Shi, D., Zhang, C., Lin, X., et al. (2019). Crosstalk between cancer cells and tumor associated macrophages is required for mesenchymal circulating tumor cell-mediated colorectal cancer metastasis. *Mol. Cancer* 18 (1), 64. doi:10.1186/s12943-019-0976-4

Wei, D., Li, C., Ye, J., Xiang, F., Xu, Y., and Liu, J. (2021). Codelivery of survivin inhibitor and chemotherapeutics by tumor-derived microparticles to reverse multidrug resistance in osteosarcoma. *Cell Biol. Int.* 45 (2), 382–393. doi:10.1002/cbin.11494

Wong, R. S. (2011). Apoptosis in cancer: from pathogenesis to treatment. *J. Exp. Clin. Cancer Res.* 30 (1), 87. doi:10.1186/1756-9966-30-87

Xiao, X., Wang, W., Li, Y., Yang, D., Li, X., Shen, C., et al. (2018). HSP90AA1-mediated autophagy promotes drug resistance in osteosarcoma. *J. Exp. Clin. Cancer Res.* 37 (1), 201. doi:10.1186/s13046-018-0880-6

Yao, J., Qin, L., Miao, S., Wang, X., and Wu, X. (2016). Overexpression of miR-506 suppresses proliferation and promotes apoptosis of osteosarcoma cells by targeting astrocyte elevated gene-1. *Oncol. Lett.* 12 (3), 1840–1848. doi:10.3892/ol.2016.4827

Yu, H., Pardoll, D., and Jove, R. (2009). STATs in cancer inflammation and immunity: a leading role for STAT3. *Nat. Rev. Cancer* 9 (11), 798–809. doi:10.1038/nrc2734

Zhang, T., Li, J., Yin, F., Lin, B., Wang, Z., Xu, J., et al. (2017). Toosendanin demonstrates promising antitumor efficacy in osteosarcoma by targeting STAT3. *Oncogene* 36 (47), 6627–6639. doi:10.1038/onc.2017.270

Zhu, K. P., Zhang, C. L., Ma, X. L., Hu, J. P., Cai, T., and Zhang, L. (2019). Analyzing the interactions of mRNAs and ncRNAs to predict competing endogenous RNA networks in osteosarcoma chemo-resistance. *Mol. Ther.* 27 (3), 518–530. doi:10.1016/j.ymthe.2019.01.001

Glossary

STAT3	signal transducer and activator of transcription 3
JAK2	janus kinase 2
miRNA	microRNA
U-2OS/Dox	doxorubicin-resistant U-2OS cells
mRNA	messenger ribonucleic acid
p-JAK2	phospho-JAK2
p-STAT3	phospho-STAT3
P-gP	P-glycoprotein
MDR1	multi-drug resistance protein 1
ABCB1	ATP-binding cassette subfamily B member 1
MRP1	multi-drug resistant associate protein 1
ABCC1	ATP-binding cassette subfamily C member 1
Bax	Bcl-2 associated X
Bcl-2	B-cell lymphoma-2
RT-qPCR	real time quantitative polymerase chain reaction
CCK8	cell counting kit-8
3′-UTR	3′-untranslated region
IC_{50}	half inhibitory concentration
RI	resistance index
NC	negative control
TCGA	the cancer genome atlas
GO	Gene Ontology
KEGG	Kyoto Encyclopedia of Genes and Genomes
BP	biological processes
MF	molecular function
CC	cellular component
FoxO	Forkhead Box O
EGFR-TKI	epidermal growth factor receptor-tyrosine kinase inhibitor
ErbB	receptor protein-tyrosine kinase
PPI	protein-protein interaction
AKT2	RAC-beta serine/threonine-protein kinase
BCL2L11	B-cell lymphoma 2-like 11
MEF2A	myocyte enhancer factor 2A
SOD2	Recombinant ruperoxide dismutase 2
FXN	Frataxin
HDAC4	Histone deacetylase 4